PHYSICAL REVIEW D **88,** 063510 (2013)

Probing dark matter couplings to top and bottom quarks at the LHC

Tongyan Lin, Edward W. Kolb, and Lian-Tao Wang

Kavli Institute for Cosmological Physics and the Enrico Fermi Institute, The University of Chicago, 5640 S. Ellis Avenue, Chicago, Illinois 60637, USA

(Received 12 May 2013; published 9 September 2013)

Monojet searches are a powerful way to place model-independent constraints on effective operators coupling dark matter to the standard model. For operators generated by the exchange of a scalar mediator, however, couplings to light quarks are suppressed and the prospect of probing such interactions through the inclusive monojet channel at the LHC is limited. We propose dedicated searches, focusing on bottom and top quark final states, to constrain this class of operators. We show that a search in mono b-jets can significantly improve current limits. The mono-b signal arises partly from direct production of b quarks in association with dark matter, but the dominant component is from top quark pair production in the kinematic regime where one top is boosted. A search for tops plus missing energy can strengthen the bounds even more; in this case signal and background have very different missing energy distributions. We find an overall improvement by several orders of magnitude in the bound on the direct detection cross section for scalar or pseudoscalar couplings.

DOI: 10.1103/PhysRevD.88.063510 PACS numbers: 95.35.+d, 95.30.Cq

I. INTRODUCTION

Production and detection of dark matter is one of the most exciting new physics opportunities at the Large Hadron Collider (LHC). The strategy to search for dark matter (DM) depends on the physics in the yet-to-be fully explored energy range of the LHC. In the maverick scenario [1], the DM is the only new particle produced and all other new particles are beyond the scale of the LHC. Then the interaction of the DM with standard model (SM) particles at these energies can be described in terms of an effective field theory (EFT).

In this case the DM signal at the LHC is missing transverse energy ($\not{E}_T$) signals such as monojets [1–6], monophotons, and related signals [4,7–10]. With an EFT description, one can classify all relevant interactions at the LHC in a straightforward way. This scenario also has the advantage that the connection between DM annihilation, direct detection, and collider signals is simple.

The ATLAS [11,12] and CMS [13,14] collaborations have published monojet constraints on the scale of new interactions in the EFT, which are then used to place constraints on the DM-nucleon scattering cross section. These constraints are most effective for DM masses below 100 GeV. Meanwhile, there has been rapid progress in the direct detection of dark matter [15,16], with the strongest bounds on DM-nucleon scattering at DM mass of around 50 GeV and for spin-independent scattering. These two approaches are complementary, and connecting them has been the focus of many recent studies [17–19].

A. Scalar operator

While the monojet search is extremely effective for many of the possible operators, it is not necessarily the optimal way to study all of them. In particular, it is challenging to constrain the scalar operator, where interactions between dark matter and quarks are mediated by a heavy scalar mediator:

$$\mathcal{O} = \frac{m_q}{M_*^3}\bar{q}q\bar{X}X, \tag{1}$$

summing over all quarks.[1] The form of the interaction is fixed by minimal flavor violation (MFV) [20]. Scalar interactions with SM quarks are typically strongly constrained by flavor changing neutral current measurements, but in MFV these dangerous flavor violating effects are automatically suppressed.

Because the interactions are proportional to quark mass, however, the monojet + $\not{E}_T$ signal rate appears to be suppressed by the light quark masses. The ATLAS monojet search based on 4.7 fb^{-1} at 7 TeV sets a limit of $M_* > 30$ GeV [11], including only couplings to charm and lighter quarks. This bound is much weaker than the constraint of $M_* > 687$ GeV for operators mediated by vector or axial interactions.

In this paper, we point out that the direct search for production of dark matter in association with third generation quarks can enhance the reach of the LHC for dark matter coupled to quarks through a scalar interaction. Direct b production gives rise to a mono-b-jet signal. We also show that the kinematics of top quark pairs plus dark matter is such that boosted tops may form the dominant contribution to the mono-b signal. However, monojet

[1]There are closely related operators, for example the pseudoscalar operator $\frac{m_q}{M_*^3}\bar{q}\gamma^5 q\bar{X}\gamma^5 X$. The collider constraints for these will be almost identical, differing only when the dark matter is heavy and produced near threshold. The direct detection cross section for these operators is velocity suppressed, however, so the best limits will come from the LHC.

searches veto on more than two hard jets, so a better strategy to probe the couplings to top quarks is the study of $t\bar{t} + \not{E}_T$ final states.

The scalar interaction has also been studied recently in Ref. [21], which showed that heavy quarks in loops can significantly enhance inclusive monojet production. We focus instead on direct identification of the heavy quarks in the final state. Mono-b final states from dark matter have also been studied in Refs. [22,23], although not in the context of MFV, so the top quark contribution to the mono-b signal was not considered.

In Sec. II we study the mono-b-jet signal where the leading jet is b tagged. This search can improve constraints on the DM-nucleon cross section, σ_n, by several orders of magnitude compared to current ATLAS limits. In Sec. III we show an even stronger limit can be obtained from a search for dark matter in association with top quarks, $t\bar{t} + \not{E}_T$. This is also the final state studied in searches for stops, supersymmetric partners to tops, and we use published results to derive limits. We find that the limit on σ_n is stronger by another factor of approximately 3 compared to the mono-b-jet search.

II. MONO-b-JET SEARCH

The scalar operator gives rise to b jets plus $\not{E}_T$ via direct b production, as well as from production of top quarks which then decay. Direct b production occurs through b and gluon-initiated processes, such as $bg \to \bar{X}X + b$; several example diagrams are shown in Fig. 1. In comparison to the light quark initial states, these processes are suppressed by the b-quark parton density. However, the enhancement due to the bottom Yukawa coupling is more than enough to compensate this.

Furthermore, $gg \to \bar{X}X + t\bar{t}$ turns out to be the dominant contribution to the monojet signal. Thus, the final states are highly b enriched. At the same time, focusing on the exclusive b-tagged final state reduces the SM backgrounds significantly. Therefore, we expect an improvement in the LHC reach for the scalar operator by requiring a b-tagged monojet.

Before presenting our results, we summarize our event simulation methods. We use MADGRAPH 5 [24] for parton-level cross sections, interfaced to PYTHIA 6 [25] for showering and hadronization, and DELPHES 2 [26] for detector simulation. For DELPHES, we set a 60% tagging efficiency for b, 10% mistag for c, and 0.2% mistag rate for light quarks and gluons [27]. Jets are clustered into $R = 0.4$ anti-k_T jets.

Up to two hard jets are allowed in the monojet and mono-b searches, so we must consider next-to-leading-order (NLO) corrections in our simulation of the signal. We generate matched samples with k_T-jet MLM matching. For SM backgrounds, we generate W/Z and $t\bar{t}$ with up to two jets. For the signal, we generate $X\bar{X}$ + jets, including up to two jets, for all flavors other than tops. Matched samples are normalized with NLO cross sections computed using MCFM [28]. We separately include $t\bar{t} + X\bar{X}$ at leading order, since a calculation of this process at NLO is not available.[2]

For the signal region we require $\not{E}_T > 350$ GeV, a leading b-tagged jet with $p_T > 100$ GeV, $|\eta| < 2.5$, and no isolated leptons. We also allow an additional softer jet, but no more than two jets with $p_T > 50$ GeV. There is a cut on the azimuthal separation between $\not{E}_T$ and the second jet, $\Delta\phi(\not{E}_T, p_T^{j_2}) > 0.4$, in order to suppress the mismeasured dijet background. This signal region overlaps well with those used in previous studies, and furthermore the dependence on the cut values appears to be mild.

The resulting cross sections at 8 TeV are given in Table I. We have split the signal into three contributions: coupling to charm and light quarks, direct b and $b\bar{b}$ production from coupling to b, and $t\bar{t}$ production.

Associated production of DM with $t\bar{t}$ constitutes the dominant signal for both monojet and mono-b signals because of the enhancement from the top mass and because of the production of boosted tops which can be tagged as b-jets. Events where only one top is boosted, and where the other top gives rise to low p_T jets, can pass the mono-b cuts. Of the events that pass the $\not{E}_T$ requirement and lepton veto, 11% survive the veto based on the p_T of the third jet and 35% of those events then have a leading jet which is b tagged. In comparison, 80% of events from direct b production survive the jet veto and about 50% of those events have a leading b-jet. Note that this assumes the same b-tagging efficiencies for the b-jets inside the boosted tops. Without dedicated study by the experimental collaborations, this is an idealized assumption. We note that most of the top jets are from mildly boosted tops, with have $p_T \approx 400$ GeV. Hence, we do not expect the b-tagging efficiency to degrade significantly. At the same time, it may be possible to use additional information to tag these jets as coming from boosted tops. We will leave this for a future study.

The dominant SM backgrounds are $Z(\nu\bar{\nu})$ + jets and W + jets, where a jet fakes a b-jet. Although these are suppressed by the mistag rate, they are still a comparable contribution to direct b production from $Z + b$ and $t\bar{t}$ backgrounds. Depending on the b-tagging algorithms used, however, it may be possible to further reduce the background from Z/W + jets.

Kinematic distributions in $\not{E}_T$ and leading jet p_T are shown in Fig. 2. The $\not{E}_T$ spectrum for b production is very similar to that for Z + jets, despite the fact that the signal arises from a contact interaction. This is partly because in the signal case, the initial states include sea quarks, while for the dominant Z + jets background

[2]The NLO corrections for the analogous process $t\bar{t} + h$ affect the cross section by 10%–20% [29,30]. For $t\bar{t} + X\bar{X}$, this would lead to a small increase in the M_* limits.

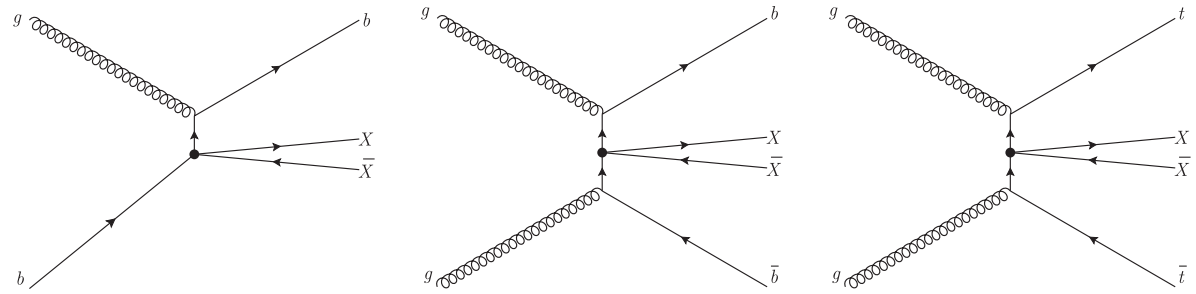

FIG. 1. Some of the dominant diagrams contributing to associated production of DM with bottom and top quarks.

roughly 70% of events are initiated by at least one valence quark. Meanwhile, $X\bar{X} + t\bar{t}$ final states tend to have more $\not{E}_T$ because of the requirement of producing massive top quarks.

To estimate the expected bound, we compute the number of signal events such that $\chi^2 < 2.71$ to obtain a 90% C.L. bound [4]. A systematic uncertainty of 5% is assumed. We also compute bounds for 14 TeV and 100 fb^{-1}, keeping the same cuts. A higher $\not{E}_T$ cut can improve bounds in the inclusive monojet case [6]; in this case, however, stronger cuts would also require higher p_T b-jets, where the b-tagging efficiency can degrade.

Figure 3 shows our constraints on M_* in the left panel and the corresponding limits for direct detection in the right panel. The scalar operator gives rise to spin-independent DM-nucleon scattering, with a cross section of

$$\sigma_n = \frac{(0.38 m_n)^2 \mu_X^2}{\pi M_*^6} \approx 2 \times 10^{-38}\ \mathrm{cm}^2 \left(\frac{30\ \mathrm{GeV}}{M_*}\right)^6, \quad (2)$$

compared to XENON100 limits of about 10^{-43} cm^2 at $m_X = 10$ GeV [15]. We find a factor of 8 improvement in σ_n limits with a mono-b search compared to an inclusive monojet search. Overall, we find a factor of 150 improvement compared to an inclusive search where only the coupling to charm quarks and lighter is considered (as in the most recent ATLAS study [11]).

TABLE I. Monojet and mono-b search at 8 TeV: Cross sections for dominant backgrounds and signal with cuts of $\not{E}_T > 350$ GeV, $p_T^{j_1} > 100$ GeV as described in the text. For the signal we take $M_* = 50$ GeV and $m_X = 10$ GeV. The row $\bar{X}X$ + jets includes only DM coupling to charm and lighter quarks. Note that $\bar{X}X + b$ + jets include single b-jet and $b\bar{b}$ production. In the column labeled b-tag, a b-tag on any jet with $p_T > 50$ GeV is required, while in the last column the leading jet must be b tagged; this choice does not lead to significantly different results in setting limits.

	Process	Monojet	b-tag	b-tag on j_1
Background	Z + jets (fake)	406 fb	8 fb	5 fb
	$Z + b$ + jet	6.7 fb	4 fb	3 fb
	W + jets, $W + b$	95 fb	3 fb	2 fb
	$t\bar{t}$ + jets	16 fb	11 fb	6 fb
Signal	$\bar{X}X$ + jets	11 fb	0.9 fb	0.7 fb
	$\bar{X}X + b$ + jets	65 fb	40 fb	33 fb
	$\bar{X}X + t\bar{t}$	120 fb	63 fb	41 fb

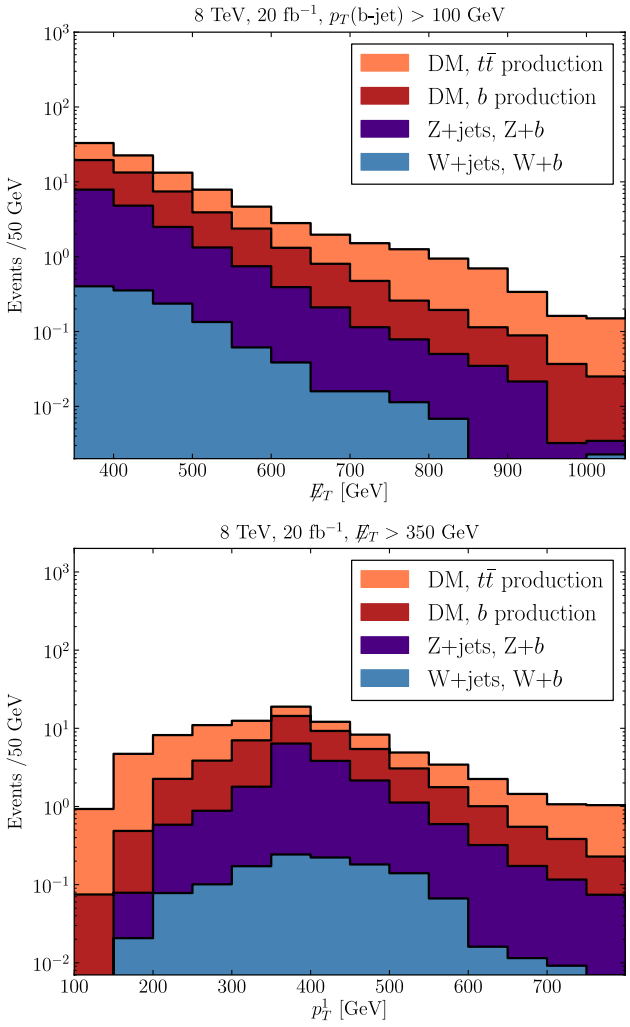

FIG. 2 (color online). Mono-b search at 8 TeV: Distributions for $\not{E}_T$ and $p_T^{j_1}$, the transverse momentum of the leading b-jet, for some of the dominant SM backgrounds and the signal. We separate the DM signal into contributions from direct b production and from $t\bar{t}$ production. For the signal we take $M_* = 50$ GeV and $m_X = 10$ GeV.

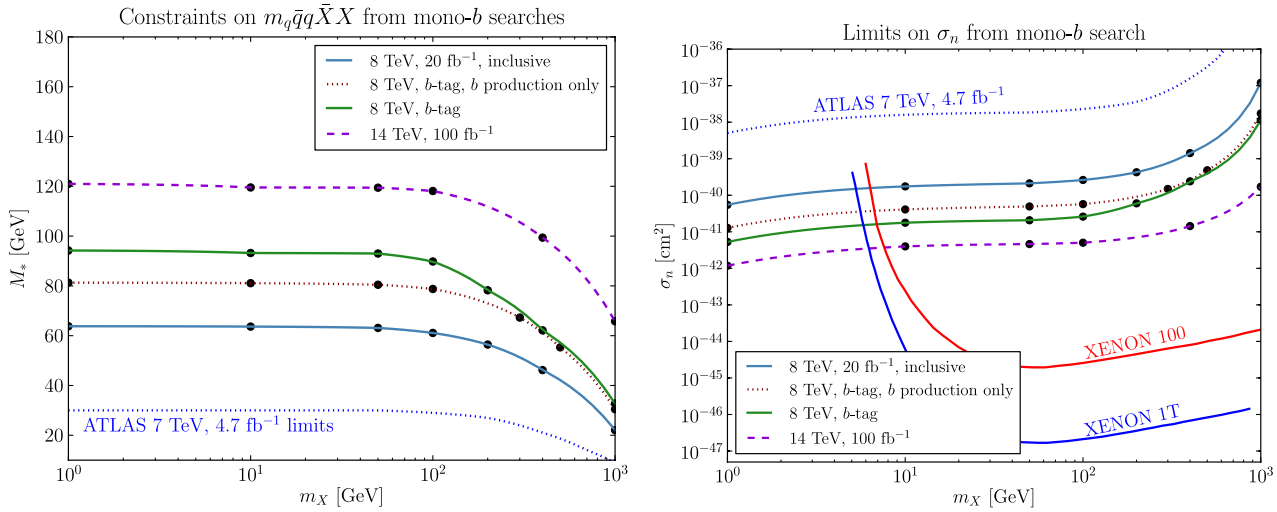

FIG. 3 (color online). (Left) Expected 90% C.L. limits on the scalar operator from a mono-b search, including couplings to tops and bottoms. For the mono-b search at 8 TeV we also show the limit if b-jets from top production are not included (dotted line). For comparison we include limits for an inclusive monojet search with no b-tag, and current ATLAS limits from [11]. (Right) Corresponding constraints on the spin-independent nucleon scattering cross section, along with XENON100 limits [15], and projected sensitivity for XENON1T [37].

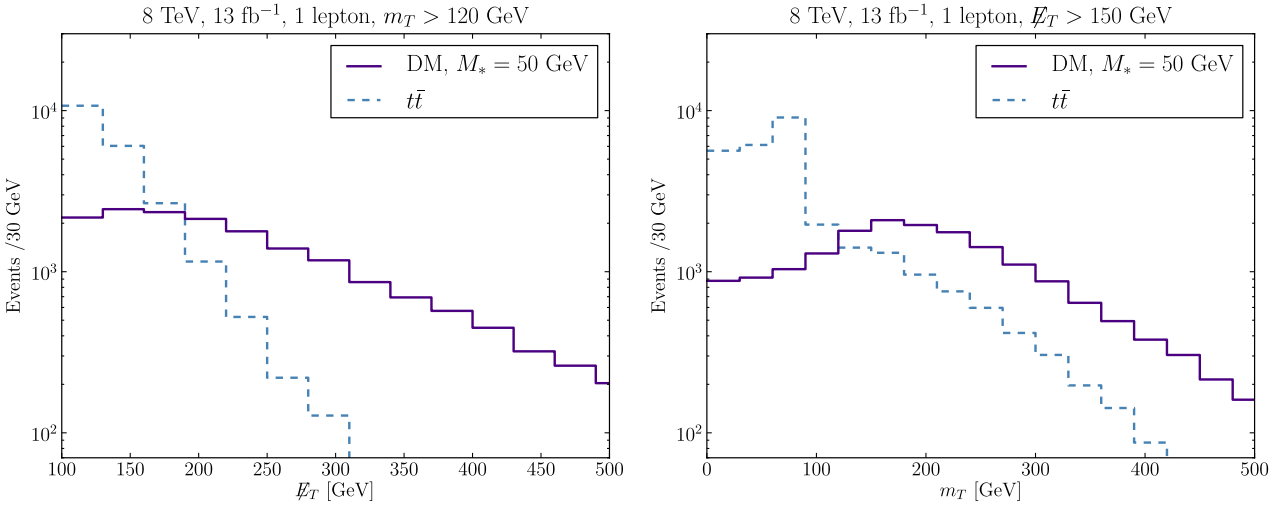

FIG. 4 (color online). (Left) $\not{E}_T$ distribution after requiring an isolated lepton and $m_T > 120$ GeV. (Right) Transverse mass m_T distribution requiring an isolated lepton and $\not{E}_T > 150$ GeV. The dark matter mass is $m_X = 10$ GeV.

III. TOPS PLUS MISSING ENERGY SEARCH

As shown in the previous section, the process $gg \to X\bar{X} + t\bar{t}$ contributes the dominant component of the monojet and the mono-b signals. The monojet and mono-b searches veto on more than two high-p_T jets, however, cutting out a large fraction of $t\bar{t}$ events. A stronger constraint on this coupling can be obtained from dedicated searches.

Models of supersymmetry also have a signature of top pairs plus missing transverse energy. We apply the recent ATLAS 8 TeV search for top-quark superpartners with 1-lepton final states [31] using 13 fb^{-1} of data to these scalar dark-matter couplings.[3] The signal regions require one isolated lepton, $\not{E}_T > 150$ GeV, transverse mass[4] $m_T > 120$ GeV, four jets with $p_T > (80, 60, 40, 25)$ GeV and at least one b-tag.

[3]We have also calculated constraints using the CMS 1-lepton final state search [32] and obtain limits that are similar although slightly weaker.

[4]The transverse mass is defined as $(m_T)^2 = 2p_T^{\rm lep}\not{E}_T(1 - \cos\Delta\phi)$ with $\Delta\phi$ the azimuthal separation between lepton and missing momentum directions.

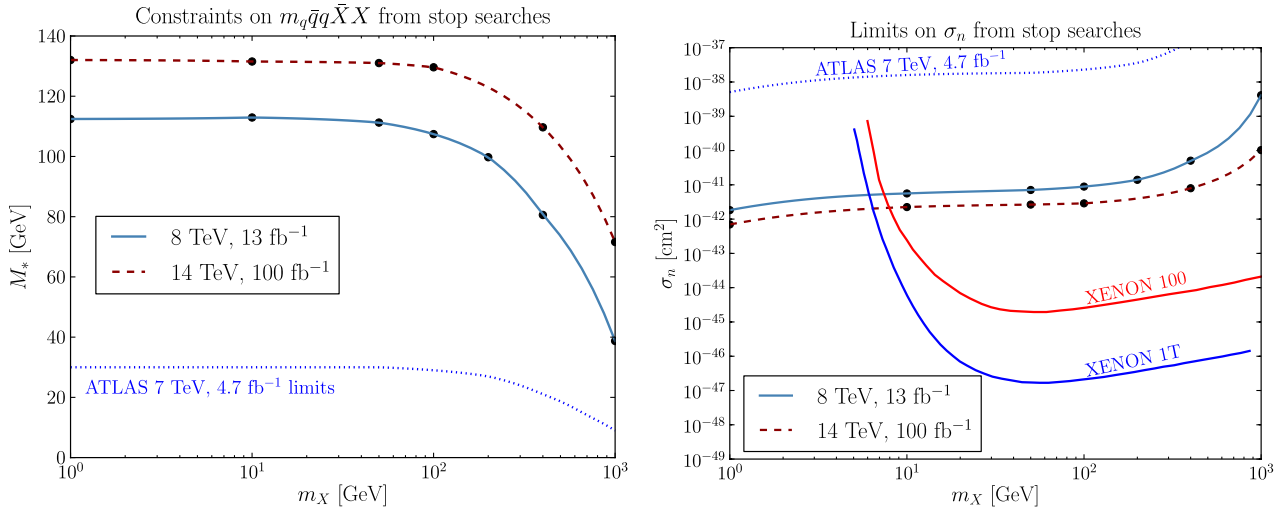

FIG. 5 (color online). (Left) Expected 90% C.L. limits on scalar operator from applying a search for supersymmetric tops with one lepton in the final state. 8 TeV limits are obtained using the results of [31]. Also shown are ATLAS limits from [11]. (Right) Corresponding constraints on nucleon scattering cross section, along with XENON100 limits [15], and projected sensitivity for XENON1T [37].

Figure 4 shows the $\not{E}_T$ and m_T distributions of the signal and the dominant background, $t\bar{t}$. The DM signal is significantly harder in the $\not{E}_T$ spectrum, whereas the background is highly peaked towards low $\not{E}_T$ because the primary source of $\not{E}_T$ is from the neutrinos in the top decay. Meanwhile, it is unlikely that stronger cuts on m_T above 120 GeV would substantially improve the ratio of signal to background.

We find the best constraints come from the signal region D (SRD) of the ATLAS study, with $\not{E}_T > 225$ GeV. Although there is another signal region with $\not{E}_T > 275$ GeV, the systematic uncertainties increase significantly. We thus apply the ATLAS SRD cuts to simulated data to derive our 13 fb^{-1} limits. The signal cross section with these cuts is

$$\sigma_{\text{signal}} = 210 \text{ fb} \tag{3}$$

assuming $M_* = 50$ GeV and $m_X = 10$ GeV. We give limits on M_* and σ_n in Fig. 5. Because uncertainties are systematics dominated for this signal region, we do not expect a significant improvement of limits with 20 fb^{-1} of data.

Figure 5 also shows limits for 14 TeV with 100 fb^{-1} of data, keeping the same cuts as above. We simulate $t\bar{t}$ for our background estimate, and assume the systematic error on the background is the same as in the 8 TeV analysis. We also calculated constraints for a search with an all-hadronic final state [33,34]; in this case it may be possible to improve the bounds on M_* by 10%–20%, depending on the detector acceptances and systematic uncertainties.

IV. DISCUSSION

We have shown that limits on scalar (and pseudoscalar) interactions of dark matter with quarks can be improved significantly by directly searching for final states with b-jets and tops. Compared to an analysis including only light quarks, we find a factor of 500 improvement in limits on σ_n, and compared to an inclusive monojet search including couplings to all quarks, we find a factor of 30 improvement. For 8 TeV data, the corresponding constraints on direct detection are below the regions favored for light dark matter interpretations of DAMA [35] and CoGeNT [36].

Couplings to heavy quarks can also lead to an enhancement of inclusive monojet production through loops; Ref. [21] found $M_* > 148^{+12}_{-11}$ GeV for small DM mass using 7 TeV data. These loop corrections were calculated assuming the same effective scalar operator considered in this paper, and leads to a stronger constraint if no signal is observed. The searches discussed here instead directly probe couplings of dark matter to heavy quark flavors. If couplings to up-type and down-type quarks are different, for example, the rates for monojets, mono-b, and dark matter plus tops will have different relations. Furthermore, the $\not{E}_T$ spectrum for the $t\bar{t}$ final state is strikingly different from the background. It may also be possible to use the difference in shapes to improve significantly on the searches discussed here.

Finally, in this paper we have assumed a contact interaction for simplicity. As discussed in Refs. [5,18], this assumption must be compared to the derived bounds on M_*. In this case, the best limit we obtain at 8 TeV is $M_* > 113$ GeV, and for this value a significant fraction of events (over 50%) violate the criteria in Refs. [5,18]. This indicates further study of UV completions of the operator is necessary. For example, in the simplest scenario one can introduce a neutral scalar mediator ϕ mediating the interactions. We then estimate the tops plus missing energy search constrains the ϕ coupling to tops to be less than 1

if $m_\phi = 100$ GeV and $m_\chi = 10$ GeV. For much lower m_ϕ the constraint weakens because the mediator is no longer produced on-shell, and for much larger m_ϕ the constraint weakens because the rate is suppressed. In general, however, the results will be more model dependent and we reserve this analysis for future work.

ACKNOWLEDGMENTS

We thank Patrick Fox, David Krohn, Bjoern Penning, Brian Shuve, and Ciaran Williams for helpful discussions, and in particular Bjoern Penning for his constant feedback. Paddy and Ciaran provided an advance copy and assistance with MCFM. E. W. K. thanks the Physics Department of the University of Rome ''La Sapienza'' and INFN, Sezione di Padova, where part of this work was completed. L. T. W. is supported by the NSF under Grant No. PHY-0756966 and the DOE Early Career Award under Grant No. desc0003930. T. L. is grateful to Perimeter Institute for their hospitality as this paper was being finished. Research at the Perimeter Institute is supported in part by the Government of Canada through Industry Canada, and by the Province of Ontario through the Ministry of Research and Information (MRI).

[1] M. Beltran, D. Hooper, E. W. Kolb, Z. A. Krusberg, and T. M. Tait, J. High Energy Phys. 09 (2010) 037.
[2] J. Goodman, M. Ibe, A. Rajaraman, W. Shepherd, T. M. P. Tait, and H.-Bo Yu, Phys. Lett. B **695**, 185 (2011).
[3] J. Goodman, M. Ibe, A. Rajaraman, W. Shepherd, T. M. P. Tait, and H.-Bo Yu, Phys. Rev. D **82**, 116010 (2010).
[4] P. J. Fox, R. Harnik, J. Kopp, and Y. Tsai, Phys. Rev. D **85**, 056011 (2012).
[5] P. J. Fox, R. Harnik, R. Primulando, and C.-T. Yu, Phys. Rev. D **86**, 015010 (2012).
[6] A. Rajaraman, W. Shepherd, T. M. Tait, and A. M. Wijangco, Phys. Rev. D **84**, 095013 (2011).
[7] P. J. Fox, R. Harnik, J. Kopp, and Y. Tsai, Phys. Rev. D **84**, 014028 (2011).
[8] Y. Gershtein, F. Petriello, S. Quackenbush, and K. M. Zurek, Phys. Rev. D **78**, 095002 (2008).
[9] F. J. Petriello, S. Quackenbush, and K. M. Zurek, Phys. Rev. D **77**, 115020 (2008).
[10] Y. Bai and T. M. Tait, Phys. Lett. B **723**, 384 (2013).
[11] G. Aad *et al.* (ATLAS Collaboration), J. High Energy Phys. 04 (2013) 075.
[12] The ATLAS Collaboration, Technical Report No. ATLAS-CONF-2012-147, 2012.
[13] S. Chatrchyan *et al.* (CMS Collaboration), J. High Energy Phys. 09 (2012) 094.
[14] The CMS Collaboration, Technical Report No. CMS-PAS-EXO-12-048, 2013.
[15] E. Aprile *et al.* (XENON100 Collaboration), Phys. Rev. Lett. **109**, 181301 (2012).
[16] Z. Ahmed *et al.* (CDMS-II Collaboration), Phys. Rev. Lett. **106**, 131302 (2011).
[17] Y. Bai, P. J. Fox, and R. Harnik, J. High Energy Phys. 12 (2010) 048.
[18] I. M. Shoemaker and L. Vecchi, Phys. Rev. D **86**, 015023 (2012).
[19] M. T. Frandsen, F. Kahlhoefer, A. Preston, S. Sarkar, and K. Schmidt-Hoberg, J. High Energy Phys. 07 (2012) 123.
[20] G. D'Ambrosio, G. Giudice, G. Isidori, and A. Strumia, Nucl. Phys. **B645**, 155 (2002).
[21] U. Haisch, F. Kahlhoefer, and J. Unwin, J. High Energy Phys. 07 (2013) 125.
[22] B. Bhattacherjee, D. Choudhury, K. Harigaya, S. Matsumoto, and M. M. Nojiri, J. High Energy Phys. 04 (2013) 031.
[23] K. Cheung, Y.-L. S. Tsai, P.-Y. Tseng, T.-C. Yuan, and A. Zee, J. Cosmol. Astropart. Phys. 10 (2012) 042.
[24] J. Alwall, M. Herquet, F. Maltoni, O. Mattelaer, and T. Stelzer, J. High Energy Phys. 06 (2011) 128.
[25] T. Sjostrand, S. Mrenna, and P. Z. Skands, J. High Energy Phys. 05 (2006) 026.
[26] S. Ovyn, X. Rouby, and V. Lemaitre, arXiv:0903.2225.
[27] G. Aad *et al.* (ATLAS Collaboration), arXiv:0901.0512.
[28] P. J. Fox and C. Williams, Phys. Rev. D **87**, 054030 (2013).
[29] R. Frederix, S. Frixione, V. Hirschi, F. Maltoni, R. Pittau, and P. Torrielli, Phys. Lett. B **701**, 427 (2011).
[30] S. Dittmaier *et al.* (LHC Higgs Cross Section Working Group), arXiv:1101.0593.
[31] The ATLAS Collaboration, Technical Report No. ATLAS-CONF-2012-166, 2012.
[32] The CMS Collaboration, Technical Report No. CMS-PAS-SUS-12-023, 2012.
[33] The ATLAS Collaboration, Technical Report No. ATLAS-CONF-2013-024, 2013.
[34] The CMS Collaboration, Technical Report No. CMS-PAS-SUS-12-028, 2012.
[35] R. Bernabei *et al.* (DAMA Collaboration and LIBRA Collaboration), Eur. Phys. J. C **67**, 39 (2010).
[36] C. Aalseth, P. Barbeau, J. Colaresi, J. Collar, J. Diaz Leon *et al.*, Phys. Rev. Lett. **107**, 141301 (2011).
[37] E. Aprile (XENON1T Collaboration), arXiv:1206.6288.